

Measurement of the $J/\psi(3100)$ Decay Widths into e^+e^- and $\mu^+\mu^-$ at Adone.

B. ESPOSITO, F. FELICETTI, I. PERUZZI, M. PICCOLO and F. RONGA

Laboratori Nazionali del CNEN - Frascati

B. BARTOLI, A. NIGRO and F. VANOLI

Istituto di Fisica dell'Università - Napoli

Istituto Nazionale di Fisica Nucleare - Sezione di Napoli

D. BISELLO and M. NIGRO

Istituto di Fisica dell'Università - Padova

Istituto Nazionale di Fisica Nucleare - Sezione di Padova

M. L. FERRER (*), A. MARINI, P. MONACELLI, L. PAOLUZI, G. PIANO-MORTARI,
F. SEBASTIANI and L. TRASATTI

Istituto di Fisica dell'Università - Roma

Istituto Nazionale di Fisica Nucleare - Sezione di Roma

(ricevuto l'8 Agosto 1975)

We report the experimental results obtained at Adone by the MEA Group on the $J/\psi(3100)$ decay into lepton pairs. Preliminary results on the integrated cross-sections for the channels $e^+e^- \rightarrow$ hadrons, $\mu^+\mu^-$, e^+e^- have been reported⁽¹⁾. In this paper we give results on the e^+e^- and $\mu^+\mu^-$ pair angular distributions and on the partial decay widths. These results turn out to be compatible with a $J^{PC} = 1^{--}$ assignment⁽²⁾ for the $J/\psi(3100)$.

(*) Supported by Accademia Nazionale dei Lincei, Roma.

(1) W. W. ASH, D. C. CHENG, B. ESPOSITO, F. FELICETTI, M. OGREEN, I. PERUZZI, M. PICCOLO, F. RONGA, G. SCHINA, G. T. ZORN, B. BARTOLI, B. COLUZZI, E. CUOMO, A. NIGRO, V. SILVESTRINI, F. VANOLI, D. BISELLO, A. MULACHIÉ, M. NIGRO, L. PESCARA, E. SCHIAPUTA, A. MARINI, P. MONACELLI, L. PAOLUZI, G. PIANO MORTARI, F. SEBASTIANI and L. TRASATTI: *Lett. Nuovo Cimento*, **11**, 705 (1974).

(2) A. M. BOYARSKI, M. BREIDENBACH, F. BULOS, G. J. FELDMAN, G. E. FISCHER, D. FRYBERGER, G. HANSON, B. JEAN-MARIE, R. R. LARSEN, D. LUKE, V. LÜTHI, H. L. LYNCH, D. LYON, C. C. MOREHOUSE, J. M. PATERSON, M. L. PERL, P. RAPIDIS, B. RICHTER, R. F. SCHWITTERS, W. TANENBAUM, F. VANNUCCI, G. S. ABRAMS, D. D. BRIGGS, W. CHINOWSKY, C. E. FRIEDBERG, G. GOLDBABER, J. A. KADYK, A. M. LITKE, B. A. LULU, F. M. PIERRE, B. SADOULET, G. H. TRILLING, J. S. WHITAKER, F. WIN-KELMANN and J. E. WESS: *Phys. Rev. Lett.*, **34**, 1357 (1975).

The Magnet Group experimental set-up (Fig. 1) is described in detail in ref. (1). We recall here briefly the angular acceptance of the experimental apparatus and the event identification criteria used in the analysis. The solid angle covered by the apparatus for pointlike source is $\Delta\Omega_c \simeq 0.4 \times 4\pi$ ($40^\circ \leq \theta \leq 140^\circ$) for momentum analysis, and $\Delta\Omega_N \simeq 0.27 \times 4\pi$ for particle identification.

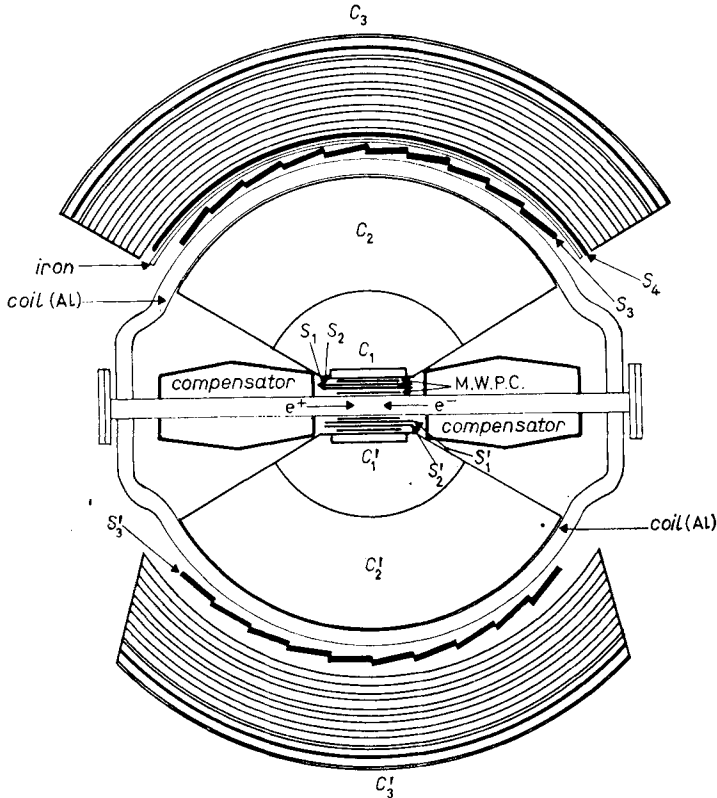


Fig. 1. - Vertical section of the experimental apparatus. C_1, C_1' are narrow-gap spark chambers; C_2, C_2' are wide-gap cylindrical spark chambers for momentum analysis; C_3, C_3' are thick-plate spark chambers for particles identification. M.W.P.C. are multiwire proportional chambers; S_1, \dots, S_4 are scintillation counters.

Events from the reaction $e^+e^- \rightarrow e^+e^-$ are identified by requiring two colinear ($\Delta\theta \leq 10^\circ$), coplanar ($\Delta\varphi \leq 10^\circ$) particles in the apparatus with opposite charges. In addition one requests

- a) the proper position of the source point;
- b) a correct timing of the event with the crossing of the e^+e^- bunches;
- c) a correct time difference in both sides of the apparatus between signals from (S_1S_2) and S_3 [$(S_1'S_2')$ and S_3'] (see Fig. 1);
- d) electromagnetic showers to be observed in the thick-plate chambers C_3, C_3' outside the magnet (see Fig. 1).

The luminosity monitor provided by the $e^+e^- \rightarrow e^+e^-$ small-angle ($(3 \div 6)^\circ$) scattering, as measured by the Adone machine group in a different interaction region of

the storage ring, was used as a relative «fast» monitor; the large-angle $e^+e^- \rightarrow e^+e^-$ scattering rate detected in the apparatus at $\sqrt{s} = 3.0$ GeV provided the absolute cross-section scale.

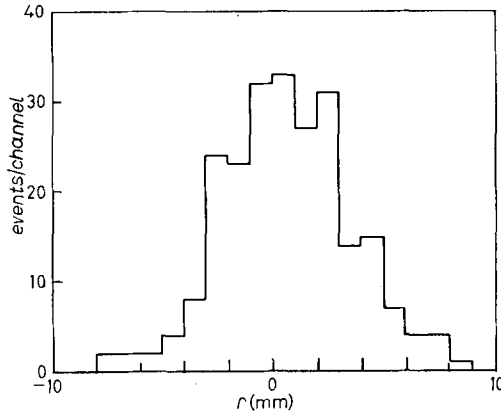


Fig. 2. - Radial source distribution of $e^+e^- \rightarrow e^+e^-$ events.

The e^+e^- results refer to an integrated luminosity $\mathcal{L} = 41.2 \text{ nb}^{-1}$ collected in the total c.m. energy interval $\sqrt{s} = (3084 \div 3125) \text{ MeV}$. The total number of $e^+e^- \rightarrow e^+e^-$ detected events is 445.

The radial source distribution of detected $e^+e^- \rightarrow e^+e^-$ events as obtained by using the information from multiwire proportional chambers is shown in Fig. 2. At Adone the radial dimension of the source is $\sim 1 \text{ mm}$. The observed $\pm 3 \text{ mm}$ spread

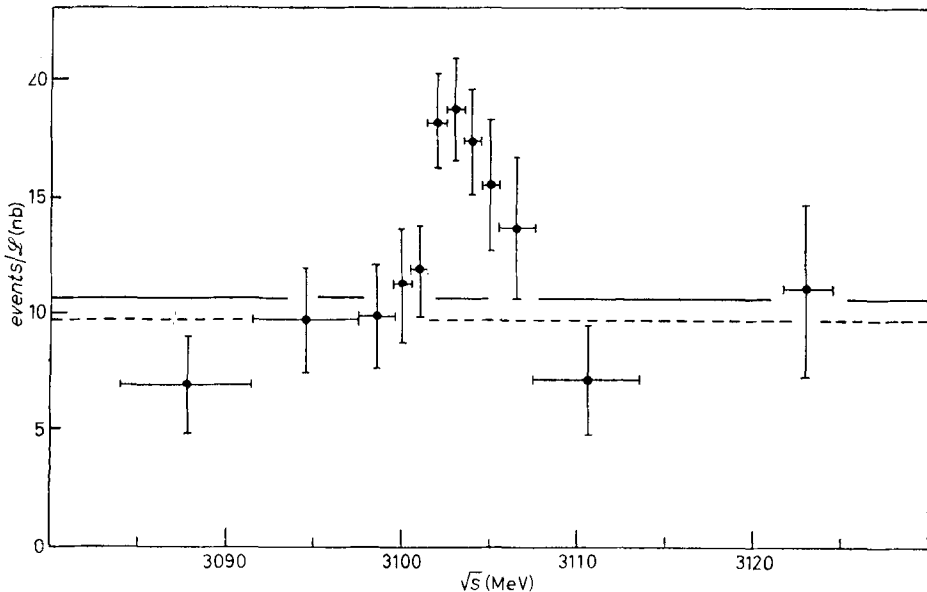


Fig. 3. - Energy dependence of $e^+e^- \rightarrow e^+e^-$ rate ($|\cos\theta| \leq 0.7$). ——— QED expected rate (Monte Carlo calculation), --- QED rate as derived from the best-likelihood fit to the angular distribution.

(F.W.H.M.) is due to wire chamber resolution and multiple scattering in the vacuum chamber walls.

The $e^+e^- \rightarrow e^+e^-$ rate integrated over the acceptance of the experimental apparatus is shown in Fig. 3 as a function of \sqrt{s} . Only e^+e^- pairs in the angular interval $|\cos \theta| \leq 0.7$ have been used in the analysis: θ is defined as the angle between the outgoing and the incoming positron. The full line in Fig. 3 shows the expected Bhabha-scattering contribution evaluated by a Monte Carlo calculation taking into account the geometrical features of the apparatus and the effect of the extended source (*). At $\sqrt{s} = 3.1$ GeV total c.m. energy the Bhabha-scattering detection efficiency of the apparatus in the angular interval $|\cos \theta| \leq 0.7$ is found to be 11%.

The angular distribution of e^+e^- pairs detected in the apparatus is given in Fig. 4a), b). Figure 4a) shows the angular distribution of events outside the resonance

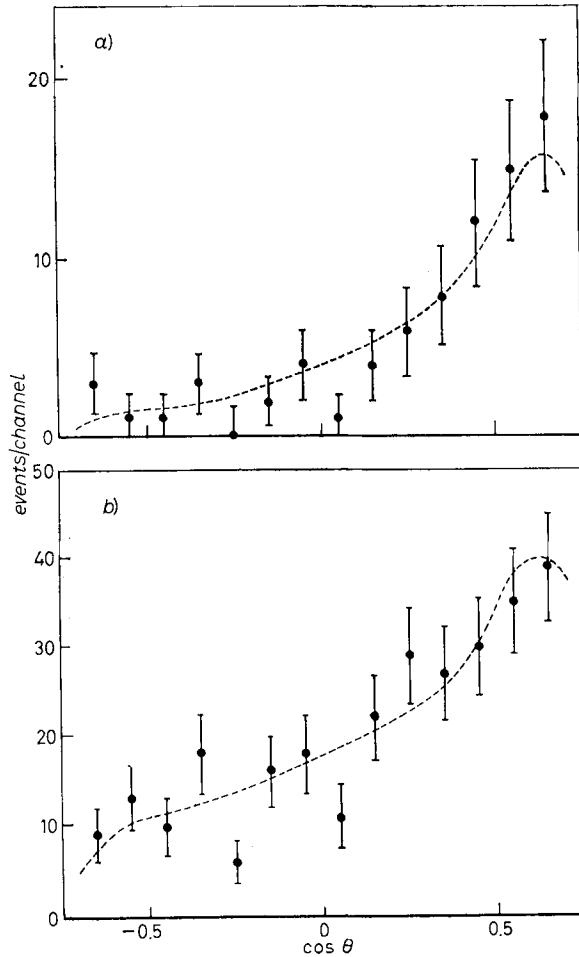


Fig. 4. - Angular distributions of detected e^+e^- pairs. The dashed lines show the behaviour obtained by the maximum likelihood calculation. Angular distribution in the energy range: a) $3.5 \text{ MeV} < |\sqrt{s} - M| < 20 \text{ MeV}$ (97% Bhabha scattering), b) $|\sqrt{s} - M| \leq 3.5 \text{ MeV}$ (59% Bhabha scattering).

(*) At Adone the longitudinal distribution of the source, $N(l)$, depends on the energy according to $N(l) = N_0 \exp[-l^2/2l_0^2]$ with l_0 (cm) = $17E_{\pm}^{\frac{1}{2}}$ (E_{\pm} , GeV).

region, $3.5 \text{ MeV} < |\sqrt{s} - M| < 20 \text{ MeV}$; Fig. 4b) shows the angular distribution inside the resonance region, $|\sqrt{s} - M| \leq 3.5 \text{ MeV}$.

The distribution of Fig. 4a) is well consistent with the expected Bhabha-scattering behaviour and that of Fig. 4b) appears to be consistent with the $1 + \cos^2\theta$ behaviour expected for a spin-one particle. We have evaluated by a maximum-likelihood procedure the relative amounts of Bhabha scattering and resonant contribution in these angular distributions. A distribution of the type

$$\alpha B(\theta) + (1 - \alpha)R(\theta)$$

has been used, where α is a free parameter and $B(\theta)$, $R(\theta)$ are the Bhabha scattering and resonant contributions respectively as seen by the apparatus. Since the energy spread of the beams is quite large with respect to the natural width of the resonance, interference effects between resonant and nonresonant contributions should be very small and have been neglected. The relative amounts of Bhabha scattering outside and inside the resonance region as determined by the maximum-likelihood calculation are given in Table I.

TABLE I.

	Energy interval (MeV)	α : fraction of Bhabha scattering	$\chi^2/\text{d.f.}$
1)	$3.5 < \sqrt{s} - 3103 < 20$	$0.97_{-0.14}^{+0.03}$	8/13
	$- 3.5 > \sqrt{s} - 3103 > -20$		
	$- 3.5 \leq \sqrt{s} - 3103 \leq 3.5$	0.59 ± 0.07	14/13
2)	$-20 < \sqrt{s} - 3103 < 20$	0.70 ± 0.06	

From the fraction $\alpha = 0.70 \pm 0.06$ (Table I, 2)) the rate of Bhabha scattering in the experimental apparatus turns out to be $(9.7 \pm 1.4) \text{ nb}$ (dashed line in Fig. 3) in good agreement with prediction of the Monte Carlo calculation which gives $(10.5 \pm 0.4) \text{ nb}$.

The $e^+e^- \rightarrow e^+e^-$ cross-sections integrated over the angular interval $|\cos\theta| \leq 0.7$ is shown in Fig. 5. The dashed line in Fig. 5 shows the energy dependence of the cross-section obtained by folding a Breit-Wigner cross-section modified for radiative correction effects⁽³⁾ with the Gaussian beam energy distribution^(*). The experimental value of the resonant total cross-section integrated over the energy interval $-3.5 \text{ MeV} < \sqrt{s} - M < 4.5 \text{ MeV}$ after having applied radiative corrections (1.52 correction factor) turns out to be

$$\sigma_I^{e^+e^-} = \int \sigma_{\text{res}}^{e^+e^-} ds^{\frac{1}{2}} = (8.2 \pm 2.2) \cdot 10^2 \text{ nb} \cdot \text{MeV}.$$

A $1 + \cos^2\theta$ angular distribution has been assumed in order to evaluate the total cross-section. By using the following equation which relates the energy integral of the

⁽³⁾ M. GRECO, G. PANCHERI-SRIVASTAVA and Y. SRIVASTAVA: *Phys. Lett.*, **56 B**, 367 (1975); M. GRECO, G. PANCHERI-SRIVASTAVA and Y. SRIVASTAVA: Frascati Report LNF-75/23(P) (1975), to be published; G. ALTARELLI, R. K. ELLIS and R. PETRONZIO: Università di Roma, Internal Report No. 612 (1975).

^(*) At Adone the energy spread of the beams at $\sqrt{s} = 3.1 \text{ GeV}$ is $\Gamma_{eB} \simeq 3 \text{ MeV}$ (F.W.H.M.).

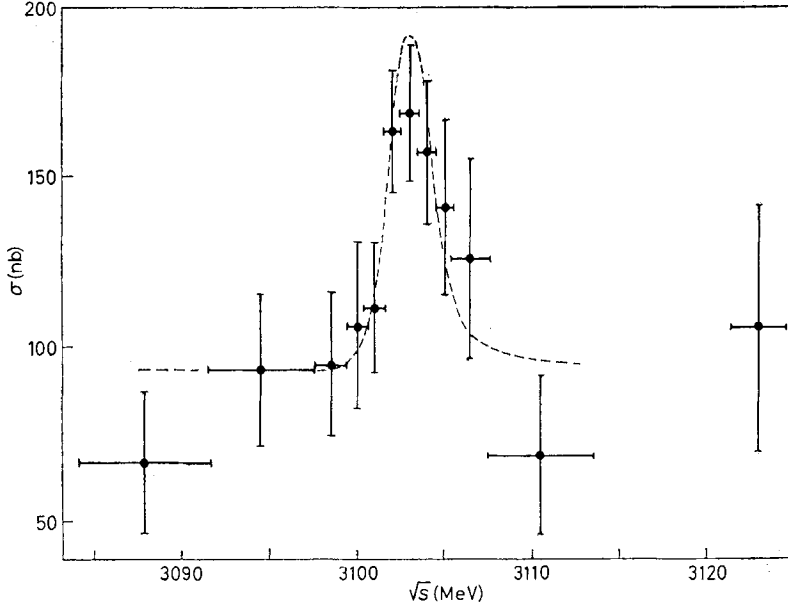


Fig. 5. - Cross-section for $e^+e^- \rightarrow e^+e^-$, integrated over the interval $|\cos\theta| \leq 0.7$, vs. the total c.m. energy.

cross-section $\sigma_I^{e^+e^-}$ to the mass and decay widths of the resonance:

$$\sigma_I^{e^+e^-} = \frac{2\pi^2(2J+1)}{M^2} \frac{\Gamma_0^2}{\Gamma_T},$$

taking $J=1$ and $M=3103$ (*), we obtain

$$\frac{\Gamma_0^2}{\Gamma_T} = (0.344 \pm 0.093) \text{ keV}.$$

The quoted error includes the systematic uncertainties in the detection efficiency and in the monitor calibration.

Events from the reaction $e^+e^- \rightarrow \mu^+\mu^-$ are requested to satisfy criteria *a*) to *c*), and in addition are identified by the absence of interactions in the thick-plate spark chambers C_3 and C'_3 (Fig. 1) and by momentum measurement. A total of 149 $\mu^+\mu^-$ events have been used in the present work in the energy interval $\sqrt{s} = (3095 \div 3108)$ MeV corresponding to an integrated luminosity $\mathcal{L} = 39.5 \text{ nb}^{-1}$. Cosmic-ray and hadron pair contaminations are completely negligible.

The angular distribution of detected $\mu^+\mu^-$ pairs integrated over the energy interval $\sqrt{s} = (3098 \div 3108)$ MeV is shown in Fig. 6. Data have been corrected for the detection efficiency of the apparatus and appear to be consistent with a $1 + \cos^2\theta$

(*) An estimate of the uncertainty in the absolute energy calibration gives an error of ± 6 MeV on the quoted J/ψ mass.

angular distribution which is also shown in Fig. 6 as a dashed line ($\chi^2/\text{degree of freedom} \approx 1.0$). The forward-backward asymmetry averaged over the energy interval $\sqrt{s} = (3098 \div 3108)$ MeV turns out to be

$$A = \frac{F - B}{F + B} = -0.03 \pm 0.09.$$

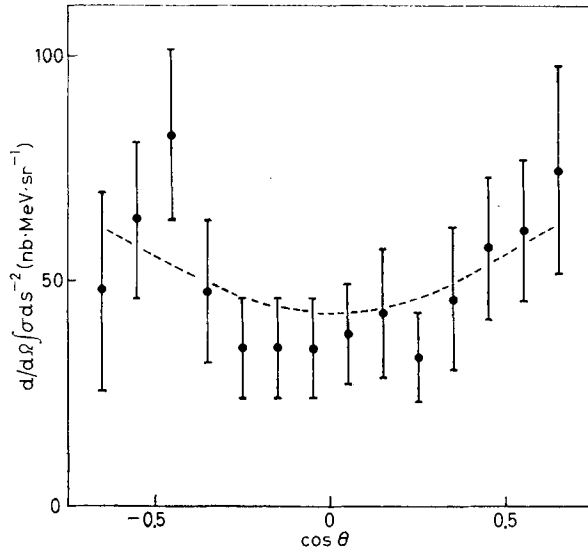


Fig. 6. - Angular distribution of $\mu^+\mu^-$ pairs integrated over the energy interval $\sqrt{s} = (3098 \div 3108)$ MeV. Data are corrected for detection efficiency. θ is the angle between the outgoing μ^+ and the incoming e^+ . The dashed line represents the $1 + \cos^2\theta$ angular distribution.

The analysis of possible energy-dependent effects on the asymmetry⁽⁴⁾ is in progress.

The $e^+e^- \rightarrow \mu^+\mu^-$ total cross-section is given in Fig. 7 as a function of the total c.m. energy \sqrt{s} . A $1 + \cos^2\theta$ angular distribution has been assumed in order to evaluate the total cross-section (5.3% geometrical detection efficiency). The full line in Fig. 7 shows the expected QED level; the dashed line shows the energy behaviour of the cross-section obtained by folding a Breit-Wigner cross-section with radiative effects and the Gaussian beam energy distribution.

The total $e^+e^- \rightarrow \mu^+\mu^-$ integrated cross-section after radiative corrections (1.56 correction factor) is found to be

$$\sigma_I^{\mu^+\mu^-} = \int \sigma_{res}^{\mu\mu} ds^{\frac{1}{2}} = (9.0 \pm 1.3) \cdot 10^2 \text{ nb} \cdot \text{MeV},$$

which gives

$$\frac{\Gamma_e \Gamma_\mu}{\Gamma_T} = (0.379 \pm 0.049) \text{ keV}.$$

(4) B. BARTOLI, D. BISELLO, B. ESPOSITO, F. FELICETTI, P. MONACELLI, M. NIGRO, L. PAOLUZI, I. PERUZZI, G. PIANO-MORTARI, M. PICCOLO, F. RONGA, S. SEBASTIANI, L. TRASATTI and F. VANOLI: Frascati Report LNF-74/64(P) (1974); G. PENSO and M. PICCOLO: Frascati Report LNF-75/15(P) (1975).

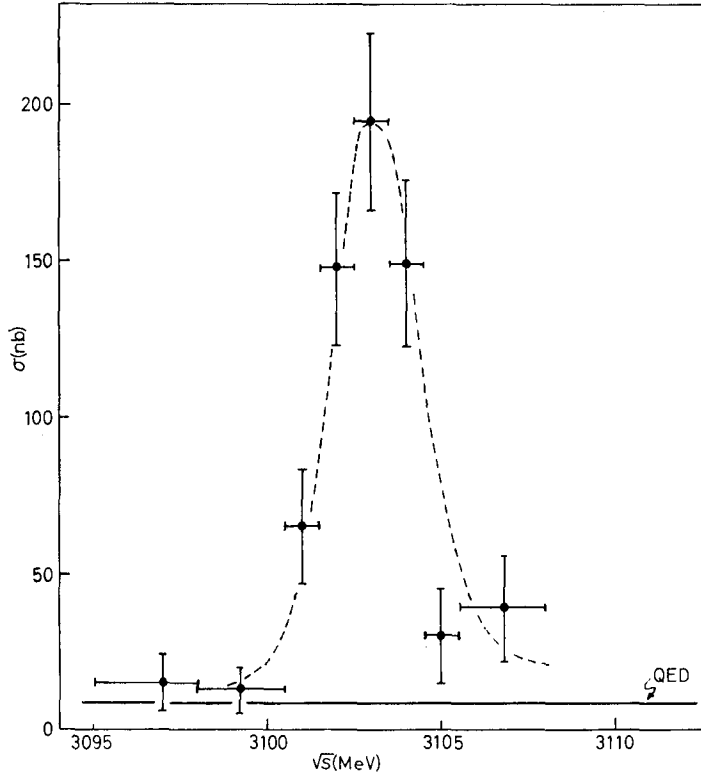


Fig. 7. - Total cross-section for $e^+e^- \rightarrow \mu^+\mu^-$ vs. the total c.m. energy. The full line shows the expected QED level.

For the ratio Γ_μ/Γ_e , we therefore obtain

$$\frac{\Gamma_\mu}{\Gamma_e} = 1.10 \pm 0.18.$$

TABLE II.

Γ_e^2/Γ_T	$= (0.34 \pm 0.09) \text{ keV}$
$\Gamma_e\Gamma_\mu/\Gamma_T$	$= (0.38 \pm 0.05) \text{ keV}$
Γ_μ/Γ_e	$= 1.10 \pm 0.18$
Γ_e	$= (4.6 \pm 1.0) \text{ keV}$
Γ_μ	$= (5.0 \pm 1.0) \text{ keV}$
Γ_H	$= (50 \pm 25) \text{ keV}$
Γ_T	$= (60 \pm 25) \text{ keV}$

The results on partial decay widths are summarized in Table II. In order to derive Γ_e , Γ_μ , Γ_{hadrons} , the value $\sigma_I^{\text{H}} = (9.2 \pm 1.9) \text{ nb} \cdot \text{GeV}$ has been used ⁽¹⁾. This value of the $e^+e^- \rightarrow J/\psi(3100) \rightarrow \text{hadrons}$ cross-section takes into account radiative corrections ⁽³⁾ (not applied in ref. ⁽¹⁾) and a more precise evaluation of multihadron detection efficiencies. Finally the results given in Table II have been obtained under the assumption $\Gamma_T = \Gamma_e + \Gamma_\mu + \Gamma_{\text{H}}$.

* * *

We wish to thank the people who worked in the early stages of this experiment. We are also extremely grateful to the Adone machine staff.